Hindawi
Shock and Vibration
Volume 2019, Article ID 2547318, 11 pages
https://doi.org/10.1155/2019/2547318

Research Article

Influence of Draft Gear Modeling on Dynamics Simulation for Heavy-Haul Train

Cheng Lei,[1,2,3] **Jia Liu**,[2] **Lisheng Dong**,[1] **and Weihua Ma**[2]

[1]*Henan Engineering Research Center of Rail Transit Intelligent Security, Zhengzhou Railway Vocational & Technical College, Zhengzhou, China*
[2]*Traction Power State Key Laboratory, Southwest Jiaotong University, Chengdu, China*
[3]*CRRC Qishuyan Co.Ltd., Changzhou, China*

Correspondence should be addressed to Weihua Ma; mwh@swjtu.edu.cn

Received 26 March 2019; Accepted 3 July 2019; Published 28 July 2019

Academic Editor: Gabriele Cazzulani

In order to study the impedance characteristics of the frictional draft gear, MT-2 draft gear is studied, and its mechanical properties are analyzed firstly. Then, the mathematical models of two common draft gears are established based on the data collected from the vehicle impact test, and the effects of the two modeling methods on the simulation results are compared through the shunting impact test and the bench test simulation. Researches show that, under various experimental conditions, the simulated draft gear characteristic curve of the lookup table model moves along a fixed trajectory regardless of the change rate of the draft gear stroke, while simulation results of the wedge-spring model depend on the change rate of the draft gear stroke and are more consistent with the experimental results, reflecting the dynamic characteristics of the draft gear and suggesting better adaptability and wider application. Finally, the "1 + 1" grouped 20,000-ton heavy-haul combined train model is established, with its draft gear characteristics under the full-braking condition on flat straight track analyzed. Calculation results and test results of the lookup table model and the wedge-spring model are compared, indicating that using the wedge-spring model to calculate the longitudinal dynamics performance is more accurate. The influence of the modeling on the longitudinal impulse simulation of the train after air braking is also studied, revealing that the variation trends of the coupler force curves of two models are basically the same, but the amplitude and frequency of the longitudinal impulse are different.

1. Introduction

The motion state of draft gear during the actual operation of train is complex and variable, and some models cannot describe the dynamic characteristics of draft gear. Most of the current researches on longitudinal dynamics only focus on the result of the impedance of draft gear. In this paper, by the simulation of relevant draft gear tests, the characteristics of impedance force-stroke for draft gears are studied, and the detailed analysis is carried out in combination with the various stages of the characteristic curve. The model is verified by tests, which can provide the basis for the dynamic characteristics of draft gear and the accurate model of vibration characteristics of coupler force.

With the increase of its running speed and the increase of axle weight and group length, the longitudinal impact force between the rolling stocks increases accordingly, and the running behavior of the coupler and draft gear devices becomes more and more complicated.

Massa et al. applied the linear draft gear model with coupler clearance to the coupler model of multibody dynamics system [1]. Cole carried out simulations and pointed out the difference in draft gear performance characteristics between train conditions and drop weight tests [2]. The model of Cheli consists of a linear spring that simulates the initial pressure, a fourth-order nonlinear spring that simulates the quasistatic response of the elastomer, two Maxwell components, and the friction components that simulates the effects of dynamic loads and high-frequency excitation as well as the effects of internal friction [3]. Geike and Melzi used the lookup table method and the fixed stiffness transition method to establish a draft gear model [4]. Hu

proposed an intelligent system model of friction-type draft gear which uses neural network technology to derive the coupler force by measurement data [5]. Jin and Luo established a draft gear model containing the peak effect measured in the shunting condition [6].

Longitudinal impulses can have different effects on the dynamics behavior of the coupler and draft gear devices as well as the dynamics performance of the train. Due to the long grouping of heavy-haul trains, the covered road section is much more complicated and the forces acting on each rolling stock are also much more complicated than those of ordinary trains. Therefore, many countries with heavy-haul transport have carried out extensive and in-depth researches on its longitudinal dynamics.

Zhai studied the calculation method of train dynamics and proposed a prediction-correction integration method and Newmark fast explicit integration method [7]; Zhang et al. proposed a new method for dynamics modeling based on the cyclic variable method, which considered the dynamics coupling relationship in longitudinal, lateral, and vertical directions, and used this model to analyze the dynamics performance of the heavy-haul trains under traction, idle running, and braking conditions, respectively [8, 9]; Sun et al. realized the numerical simulation of vehicle impact by cosimulation method [10]; Wei and Lin carried out studies on the longitudinal dynamics of the train by using air-braking characteristics simulation based on gas flow theory and using longitudinal dynamics simulation based on rigid body dynamics and proposed a series of measures to improve the longitudinal impulse of the train [11]; Belforte et al. established a more simplified air-braking model in order to better combine the fluid system model and the longitudinal dynamics model of the train [12]; Wu et al. optimized the modeling of the draft gear and studied the influence of longitudinal impulse on heavy-haul trains from the perspective of coupler fatigue based on the characteristics of the draft gear [13, 14]; and Sun et al. studied the energy consumption of trains on a typical heavy-haul line [15].

Recently, the international benchmarking of longitudinal train dynamics simulators evaluated nine longitudinal dynamics simulation software from six countries [16]. Results show that all software simulations of locomotive traction/braking force, train resistance, and track gradient are basically the same, while the main difference lies in the use of the draft gear model, which leads to subtle differences in the simulation results of the longitudinal forces, but in general, similar longitudinal force results can be obtained. The simulation of both the dynamic and static characteristics of the draft gear is of great significance, and it also has a great influence on the reliability of the longitudinal dynamics model. Therefore, attention should be paid to the response accuracy of the impedance characteristic of the draft gear during modeling. Traditionally, it is believed that different draft gear modeling has a significant impact on the longitudinal dynamics simulation of trains. However, only the longitudinal forces are examined in the evaluation, and the performances of the draft gear model in shunting impact test and bench tests are not considered. Thus, it is necessary to do a more in-depth comparative analysis on this basis.

2. Draft Gear Modeling

2.1. Working Principle of Frictional Draft Gear. Draft gear combining MT-2 steel spring and dry friction absorbs the impact mainly by the friction wedge, the damper spring, and the return spring. According to the assembly and motion relationship of each component of the draft gear, its working process can be simplified into four stages [17], namely, loading phase I, loading phase II, unloading phase I, and unloading phase II, as shown in Figure 1.

During the loading phase I, the slave plate and the center wedge move under compression, but the moving plate is not yet in motion. At this phase, the energy consumption of draft gear is mainly caused by the friction between the wedge and the center wedge, the fixed inclined plate as well as the centering spring seat. During the loading phase II, the slave plate, the center wedge, and the moving plate will move together, and the friction consists of the relative friction between the moving plate and the fixed outer plate as well as the fixed inclined plate in addition to the abovementioned wedge friction. During the unloading phases, the working mechanism of the draft gear is similar to that of the loading phases.

2.2. Analysis of Mechanical Properties of the Draft Gear. Analysis is conducted on the relative motion of and applied force on the friction surfaces of the wedge. When the center wedge moves in the longitudinal direction relative to the box, the wedge has relative displacement to the center wedge, the fixed inclined plate as well as the centering spring seat. If the center wedge moves x_1 in the longitudinal direction, the wedge moves x_2 in the longitudinal direction, and the centering spring seat moves x_3 in the longitudinal direction, while the relative displacement between the wedge and the fixed inclined plate is δ_1, the relative displacement between the center wedge and the wedge is δ_2, and the relative displacement between the wedge and the centering spring seat is δ_3. The relationship between the angle and displacement of each friction surface is shown in Figure 2.

According to the displacement vector triangle of each friction surface shown in Figure 2(b), the displacement relationship between the center wedge, the wedge, and the centering spring seat can be obtained:

$$\begin{cases} x_2 = \dfrac{1}{1-\tan\alpha\,\tan\gamma}x_1, \\ x_3 = \dfrac{1+\tan\beta\,\tan\gamma}{1-\tan\alpha\,\tan\gamma}x_1, \\ \delta_1 = \dfrac{\cos\alpha}{\cos(\alpha+\gamma)}x_1, \\ \delta_2 = \dfrac{\sin\gamma}{\cos(\alpha+\gamma)}x_1, \\ \delta_3 = \dfrac{\cos\alpha\,\sin\gamma}{\cos(\alpha+\gamma)\cos\beta}x_1, \end{cases} \tag{1}$$

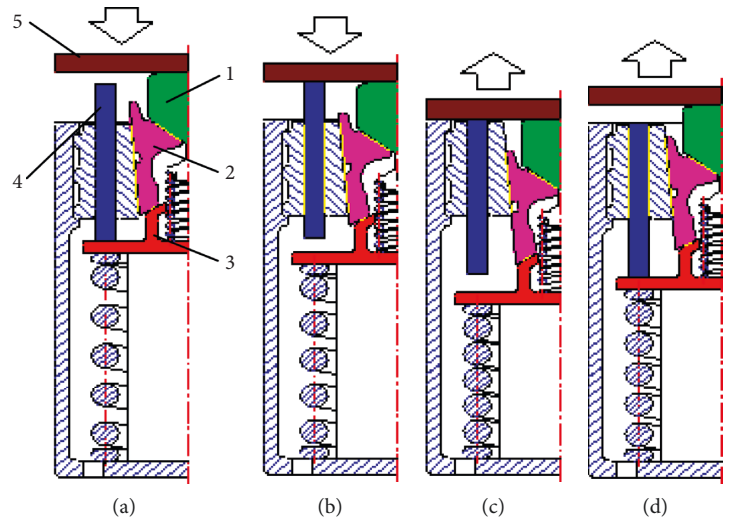

Figure 1: Working principle of MT-2 draft gear. (a) Loading phase I. (b) Loading phase II. (c) Unloading phase I. (d) Unloading phase II. 1, center wedge; 2, wedge; 3, centering spring seat; 4, moving plate; 5, slave plate.

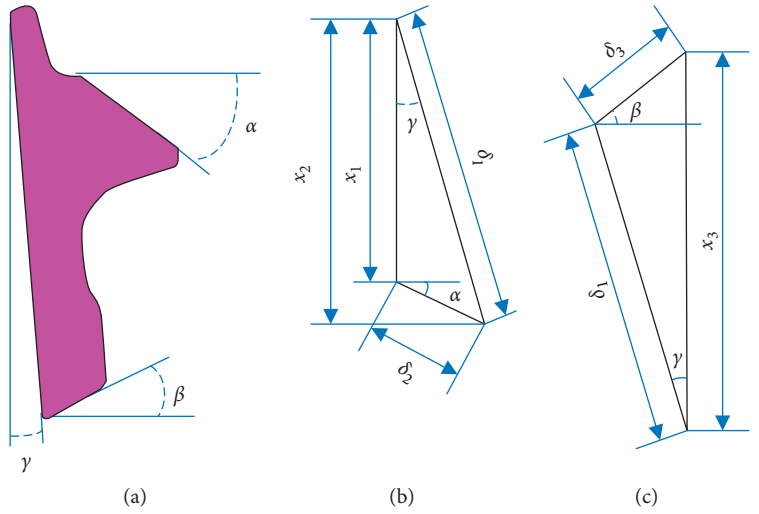

Figure 2: (a) Angle and (b) displacement of each friction surface.

where α is the angle between the friction surface of the center wedge and the cross section of the draft gear; β is the angle between the friction surface of the wedge and the centering spring seat and the cross section of the draft gear; and γ is the angle between the friction surface of the wedge and fixed inclined plate and the longitudinal section of the draft gear.

It can be seen that the displacement of each component of the draft gear and the relative displacement of the friction surfaces can be expressed by x_1, and the tensile or compressive displacement of the main spring and the return spring can also be expressed as

$$\begin{cases} x_{sm} = \dfrac{1 + \tan\beta \tan\gamma}{1 - \tan\alpha \tan\gamma} x_1, \\ x_{sr} = \left(1 - \dfrac{1 + \tan\beta \tan\gamma}{1 - \tan\alpha \tan\gamma}\right) x_1, \end{cases} \tag{2}$$

where x_{sm} is the tensile or compressive displacement of the main spring, namely, the longitudinal displacement of the centering spring seat relative to the box, and x_{sr} is the tensile or compressive displacement of the return spring, namely, the longitudinal displacement of the central wedge and the centering spring seat.

Assuming that the relative motion of the friction surfaces inside the draft gear is always in a slow and stable dynamic friction state, the quasistatic analysis of the four typical working phases of the draft gear can be conducted by the force balance condition. When the draft gear is under static pressure, the relationship between forces acting on it and displacement is shown in Figure 3, where α, β, and γ are 37°, 26°, and 4°, respectively, and the friction coefficient of each friction surface is 0.3.

2.3. Model of the Coupler and Draft Gear. In actual train shunting or working conditions, the draft gear often has a spike effect at the end of loading and at the beginning of unloading, which is caused by the change of friction coefficient with speed. In these two phases, the relative sliding

speed of each friction surface is low, that is, the frictional motion is in a weakly locked state, and the friction coefficient after locking is significantly larger than that at the time of sliding, thereby causing an abrupt change in the resistance force of the draft gear, which makes its modeling more difficult.

For the sake of longitudinal dynamics simulation, the vehicle connection system is usually simplified to a unit model, so the draft gears of two adjacent vehicles are modeled in series as one unit. In addition, a complete model should also include the gap element, the initial pressure, and the transition characteristics of the loading and unloading curves.

2.3.1. Lookup Table Model. The lookup table method is the most widely used method to establish the impedance of the draft gear stroke characteristics. The loading and the unloading characteristic curves can be obtained according to the fitting results of the draft gear-related experiment (drop hammer or shunting impact), while the gap element, the initial pressure, and the rigid contact are simultaneously taken into account. The gap between loading and unloading is handled by a fixed stiffness. The mathematical expression of the model is given by the following equations [18]:

$$F(x_t, v_t) = \begin{cases} f_l(x_t) x_t v_t \geq 0, \\ f_u(x_t) x_t v_t \leq 0, \end{cases} \tag{3}$$

$$F(x_t, v_t) = F(x_{t-\Delta t}, v_{t-\Delta t}) + k(x_t - x_{t-\Delta t}), \tag{4}$$

$$|f_u(x_t)| \leq |F(x_t, v_t)| \leq |f_l(x_t)|, \tag{5}$$

where F is the impedance force of the draft gear; θ and θ are the stroke of the current step and the previous step of the draft gear, respectively; θ and θ are the deformation speed of the current step and the previous step of the draft gear, respectively; f_l and f_u are the loading and unloading characteristic functions of the draft gear; and k is the transitional characteristic stiffness.

Equation (3) is obtained by directly interpolating from the loading or unloading curve according to different conditions, and equation (4) is used to calculate the restoring force of the draft gear on the transition curve. The value obtained from the transition curve must be corrected by the loading and unloading curves of the draft gear as a boundary condition according to equation (5) in order to obtain the correct impedance of the draft gear.

2.3.2. Wedge-Spring Model. The frictional draft gear can be simplified into a system consisting of a spring and a wedge as shown in Figure 4, wherein the wedge angle θ acts to convert the longitudinal force of the draft gear into a normal force on the friction surface, thereby introducing friction into the model [2].

According to the analysis of forces acting on the draft gear during operation, the matrix equations for loading and unloading can be obtained:

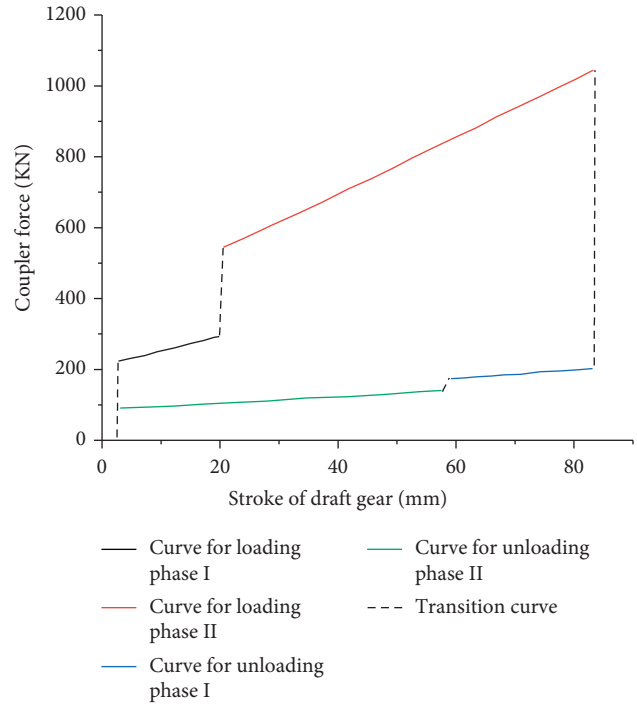

Figure 3: Draft gear characteristic curve under static pressure.

$$\text{loading}: \begin{bmatrix} \cos\theta & 0 & -\sin\theta & 0 & 0 \\ \sin\theta & -1 & \cos\theta & 0 & 0 \\ 0 & \sin\theta & 0 & 0 & -1 \\ 0 & \cos\theta & 0 & -1 & 0 \\ 0 & 0 & 0 & \mu & -1 \end{bmatrix} \begin{bmatrix} F \\ F_{N_1} \\ F_{N_2} \\ F_{N_3} \\ f \end{bmatrix} = \begin{bmatrix} 0 \\ 0 \\ F_s \\ 0 \\ 0 \end{bmatrix},$$

$$\text{unloading}: \begin{bmatrix} \cos\theta & 0 & -\sin\theta & 0 & 0 \\ \sin\theta & -1 & \cos\theta & 0 & 0 \\ 0 & \sin\theta & 0 & 0 & 1 \\ 0 & \cos\theta & 0 & -1 & 0 \\ 0 & 0 & 0 & \mu & -1 \end{bmatrix} \begin{bmatrix} F \\ F_{N_1} \\ F_{N_2} \\ F_{N_3} \\ f \end{bmatrix} = \begin{bmatrix} 0 \\ 0 \\ F_s \\ 0 \\ 0 \end{bmatrix}, \tag{6}$$

where F_{N_1} is the pressure between the two wedges, F_{N_2} and F_{N_3} are the pressures of the box to the wedge, f is the friction of the wedge, θ is the angle of the wedge, μ is the friction coefficient, Δx is the stroke change of the draft gear, and F_s is the spring force.

The draft gear impedance force-stroke characteristics including the coupler gap, initial pressure, and rigid contact can be fitted by the nonlinear spring force F_s to establish the wedge-spring model, and the expression of its impedance can be obtained by

$$F(x_t, v_t) = \begin{cases} F_s(\Delta x) \dfrac{\tan\theta}{\tan\theta - \mu(v_t)} \Delta x \geq 0, \\ F_s(\Delta x) \dfrac{\tan\theta}{\tan\theta + \mu(v_t)} \Delta x < 0. \end{cases} \tag{7}$$

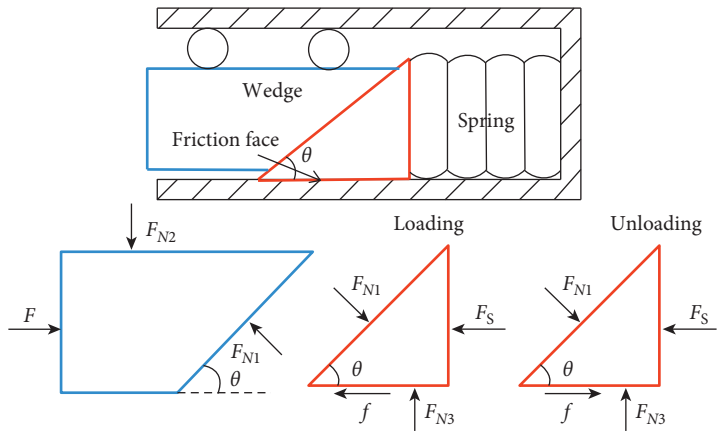

Figure 4: Simplified model of frictional draft gear and analysis of forces applied.

Based on the abovementioned, impact test data are collected and a lookup table model is established by having a 93 t wagon impacting another stationary wagon of the same quality at an initial speed of 8 km/h, and then the main spring force of the wedge-spring model is corrected. The comparison between the simulation results of the two models and the experimental results is shown in Figure 5.

According to the expression of the wedge-spring model, the friction angle of the draft gear, θ, and the friction parameter, etc., are input in the TDEAS software before the simulation. The friction coefficient can be expressed as

$$\mu = h_1 + h_2 \exp\left[-h_3 \mathrm{abs}\,(v)\right]. \tag{8}$$

In the expression, h_1 determines the dynamic friction coefficient; $h_1 + h_2$ determines the static friction coefficient; and h_3 determines the conversion process from static friction to dynamic friction. The difference between calculating speeds of the two models is not significant.

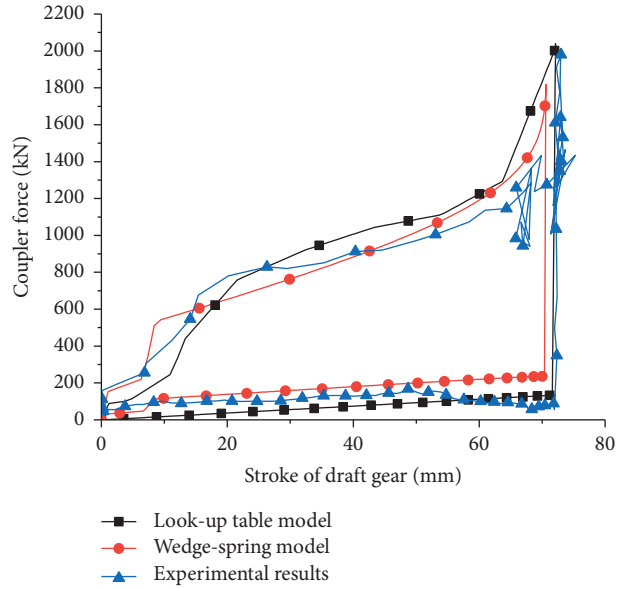

Figure 5: Simulation results of the two models and comparison of experimental results.

3. Simulation of the Draft Gear Characteristics

3.1. Shunting Impact Test. The vehicle impact test can simulate the working conditions of the vehicles impacting at different relative coupling speeds. Through this test, the cushioning and energy absorption limits of the draft gear and the longitudinal bearing capacity of the vehicle body structure can be evaluated. Both the impact vehicle and the impacted vehicle are wagons with a weight of 93 t, equipped with MT-2 frictional draft gear. The impact vehicle slides down from a certain slope and height to obtain the required initial speed and impacts the other vehicle parked on a flat straight road.

The simulation of the shunting impact is based on the establishment of the dynamics differential equations of both vehicles. Since the wagon has no traction and electric braking force, air braking is excluded from consideration and only the basic resistance of the vehicle and the draft gear at the impact end needs modeling. The longitudinal dynamic differential equations of the two vehicles are as follows:

$$\begin{cases} m_1 \ddot{\delta}_1 = -F_1 - F_{1r}, \\ m_2 \ddot{\delta}_2 = -F_2 - F_{2r}, \end{cases} \tag{9}$$

where m_1 and m_2 are the mass of the impact vehicle and the impacted vehicle, $\ddot{\delta}_1$ and $\ddot{\delta}_2$ are the acceleration of the impact vehicle and the impacted vehicle, F_1 and F_2 are the impedance force of draft gears of the impact vehicle and the impacted vehicle, and F_{1r} and F_{2r} are running resistance of the impact vehicle and the impacted vehicle, respectively.

3.1.1. Shunting Impact Simulation with Lookup Table Model. The draft gears of the two impact wagons are all based on the lookup table models, which are simulated with different initial velocities. The comparison of simulation and test data from the first complete loading and unloading cycle is shown in Figures 6(a)–6(c).

It can be seen from the experimental data that as the impact velocity increases, the coupler force and the draft gear stroke of the impacted vehicle increase; the loading process of the draft gear is obviously divided into two phases, with different stiffness at different phases and a spike effect at the end of the loading curve, all of which are consistent with the results obtained by theoretical analysis. The simulations agree well with the experimental curves at different initial velocities, and the strokes of the draft gears are basically the same, but the simulation curves at three impact velocities of 4 km/h, 6 km/h, and 7 km/h do not show spikes at the end of the loading process, with the maximum coupler force smaller than the actual value. The 8 km/h shunting impact is fitted to the experimental data according to the impact velocity, and the curve can better reflect all the characteristics of the draft gear. The analysis shows that the lookup table model can reflect the behavior of the frictional draft gear within a certain range, despite some limitations.

Figure 6(d) shows a comparison of the simulation results of lookup table models at the different initial velocities under the shunting impact conditions. It can be seen that the loading and unloading of the draft gear are developed along the same trajectory at each speed, the impact velocity only affects the stroke of the draft gear, and there is a spike effect only at an impact velocity of 8 km/h.

3.1.2. Shunting Impact Simulation with the Wedge-Spring Model. The draft gear model is changed into the wedge-spring model, and the same wagon with a mass of 93 t is simulated and conducted to impact the other stationary wagon of the same mass at different initial velocities. The comparison between the simulation results of the models and the experimental results from the first complete loading and unloading cycle is shown in Figures 7(a)–7(c).

Comparing the simulation results of the wedge-spring model with the experimental values, we can see that both the draft gear stroke and the maximum coupler force are close other at different initial impact velocities, and the curves are in good agreement, indicating that the wedge-spring model can well reflect the behavior of frictional draft gear. Figure 7(d) shows a comparison of the simulation results at different initial velocities under the shunting impact condition, indicating that the trajectories are different at different velocities, suggesting the relationship between the draft gear impedance force-stroke characteristics and the relative speed of the vehicle. The simulation results of this model are more in line with the dynamic nature of the draft gear, with spikes all reflected at the end of the loading process.

3.2. Bench Test Simulation. Bench test is conducted by fixing the draft gear on the experimental bench, with sinusoidal excitation of a certain amplitude and frequency applied to the draft gear. The expression is as follows:

$$\begin{cases} y = A\sin(2\pi f \cdot t), \\ \dot{y} = 2\pi f A\cos(2\pi f \cdot t), \end{cases} \tag{10}$$

where y is the displacement of the draft gear, $\dot{y}$ is the change rate of the draft gear stroke, A is the amplitude, and f is the frequency.

Different draft gear models are used to simulate bench tests with fixed frequency of 10 Hz and different amplitudes, and with fixed amplitude of 20 mm and different frequencies, respectively. The experimental parameters are shown in Table 1. At the same frequency, the larger the amplitude is, the larger the maximum change rate of the draft gear stroke is, and at the same amplitude, the larger the frequency is, the larger the maximum change rate of the draft gear stroke is.

3.2.1. Bench Test Simulation with Lookup Table Model. The lookup table model is adopted. The initial displacement is set at 40 mm and frequency at 10 Hz, and the simulation results of different amplitudes are shown in Figure 8(a). It can be seen from the figure that the characteristic curves of the draft gear at different amplitudes in one cycle all form a closed loop. The larger the amplitude is, the larger the loop is, and the characteristic curves at different amplitudes follow the same trajectory while loading and unloading.

Adjust the simulation parameters: the initial displacement is also 40 mm, yet the amplitude is 20 mm, and the simulation results of different frequencies are shown in Figure 8(b). As shown in the figure, the characteristic curves of the four frequencies coincide, indicating that the simulation results of the bench test using lookup table model are independent of the vibration frequency, and the simulation results are basically in line with the curve of the 8 km/h shunting impact test.

3.2.2. Bench Test Simulation with the Wedge-Spring Model. Simulation parameters are set as follows: the initial displacement is 40 mm and the frequency is 10 Hz, and the simulation results of different amplitudes are shown in Figure 9(a). As we can see from the figure, as the amplitude increases, the coupler force of the draft gear characteristic curve decreases in the same displacement interval. This is because the larger the amplitude is, the larger the maximum change rate of the draft gear stroke is, and the characteristic curve of the draft gear changes.

Adjust the simulation parameters: the fixed amplitude is 20 mm, and the simulation results of different frequencies are shown in Figure 9(b). It can be seen from the figure that in the stroke interval (20 mm and 60 mm), the coupler force of the draft gear characteristic curve decreases with the increase of frequency; the smaller the frequency is, the smoother the curve is; but the simulation results of different frequencies reveal the same maximum coupler force at stroke of 60 mm. The draft gear characteristic curve at the frequency of 15 Hz is closest to the curve of the 8 km/h impact test because the dynamic behaviors of the draft gears are the closest in the simulated stroke interval.

4. Analysis of Train Braking Conditions

This paper establishes a longitudinal dynamics model based on the HXD1"1 + 1" grouped 20,000-ton heavy-haul

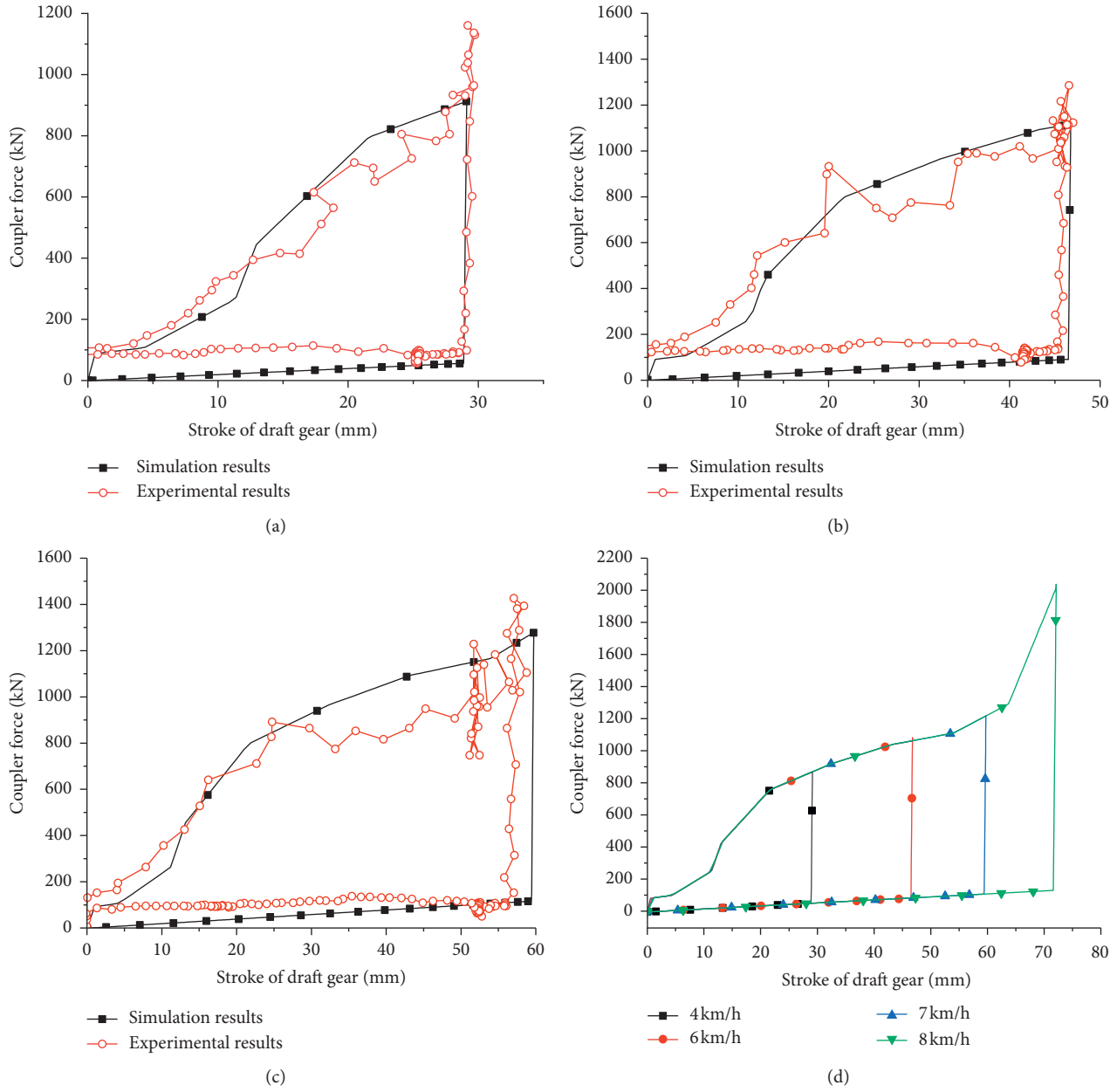

Figure 6: Shunting impact simulation with the lookup table model and comparisons of simulation results. (a) 4 km/h shunting impact simulation and test results. (b) 6 km/h shunting impact simulation and test results. (c) 7 km/h shunting impact simulation and test results. (d) Comparison of the simulation results at different initial velocities.

combined train of Shuohuang Railway, namely, 1 main control locomotive +105 C_{80} wagons +1 slave locomotive +105 C_{80} trucks + controllable train tail, with the wagon equipped with MT-2-type draft gear, and the locomotive adopting QKX-100 draft gear. The main parameters are shown in Table 2.

4.1. Full Braking on Flat Straight Track. 170 kPa is applied to 20,000-ton heavy-haul train to have full-braking stop on flat straight track. Simulation results are shown in Figure 10. It can be seen from Figure 10(a) that the two models share similarity in that the calculated train speed is changing with the braking time and the distance. The braking time and distance calculated from the wedge-spring model are smaller, although it is not a significant difference. It can be seen from Figure 10(b) that calculation results of the two models both show a large coupler force in the middle-rear part of the train and a consistency in the number of wagon where the maximum coupler force is generated, but for the lookup table model, the coupler force acting on the train is relatively smaller.

Table 3 shows a comparison of the 170 kPa full-braking simulation results and the test results. It can be seen from the data in the table that the calculation results of the train braking time, the maximum coupler force, and the number of wagon where the maximum coupler force is generated

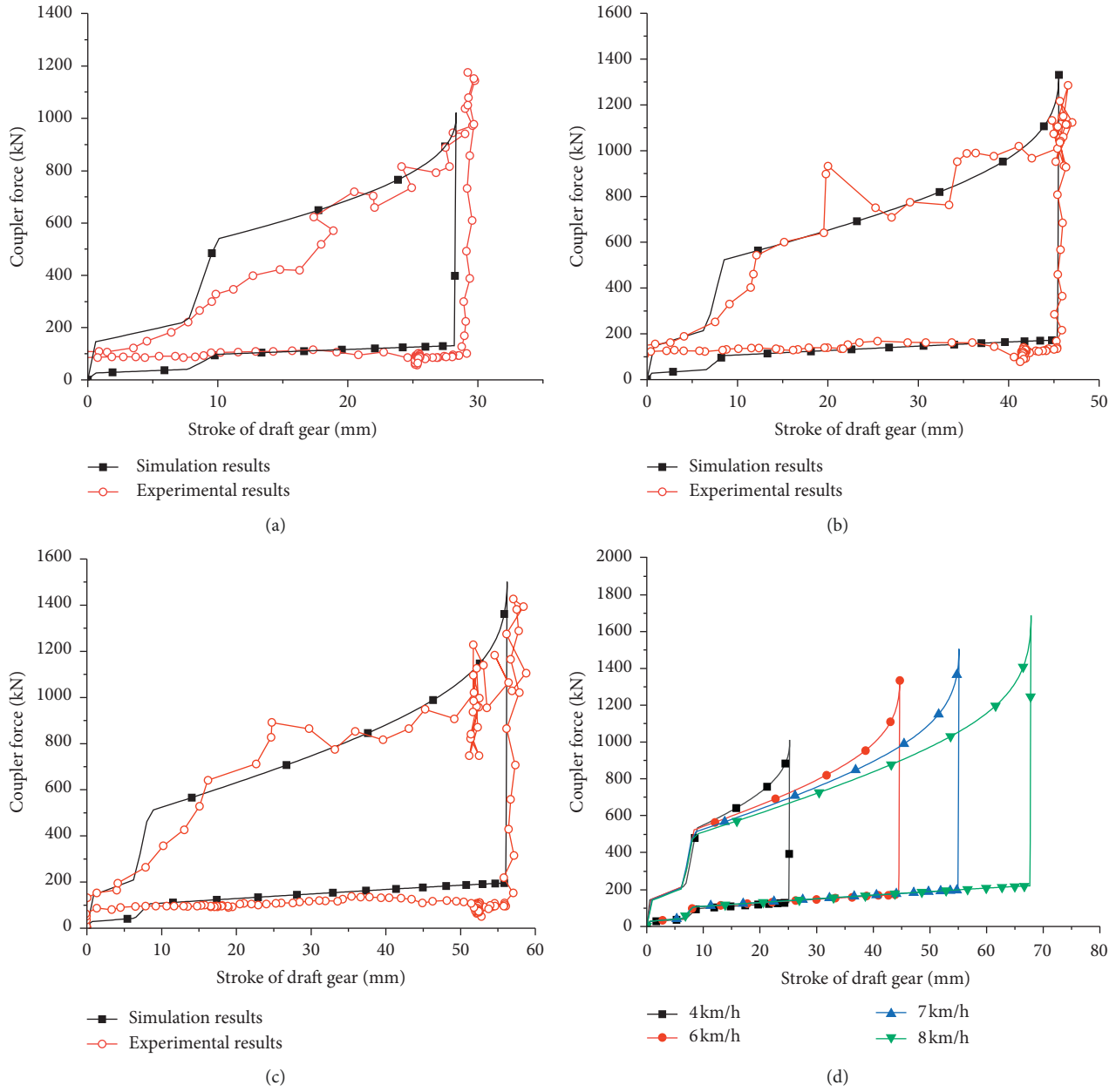

Figure 7: Shunting impact simulation with the wedge-spring model and comparisons of simulation results. (a) 4 km/h shunting impact simulation and test results. (b) 6 km/h shunting impact simulation and test results. (c) 7 km/h shunting impact simulation and test results. (d) Comparison of the simulation results at different initial velocities.

Table 1: Experimental parameters.

Frequency, 10 Hz	Amplitude (mm)	5	10	15	20
	Maximum velocity of draft gear (km/h)	1.13	2.26	3.29	4.52
Amplitude, 20 mm	Frequency (Hz)	1	5	10	15
	Maximum velocity of draft gear (km/h)	0.45	2.26	4.52	6.79

from the wedge-spring model are closer to the test values, while the braking distance of the lookup table model is closer to the test value, although the two models are not much different. It follows that for the simulation of full-braking conditions, using the wedge-spring model is more accurate to calculate the longitudinal dynamics performance.

4.2. Downhill Cycle Braking. The time course of the coupler force within the 250 s before and after the air brake is initiated is analyzed to study the vibration characteristics of coupler force during the longitudinal impulse of the train. Figure 11 shows the time course of the coupler force of the 108th wagon after a 50 kPa decompression air brake. When

Table 2: Main parameters of the model.

Main parameters	
Wagon weight	100 t
Locomotive weight	2 × 100 t
Wagon number	210
Lag time of slave locomotive	3.5 s
Coupler gap	10 mm
Locomotive dynamic braking force	461 kN
Locomotive starting traction force	760 kN
Track adhesion coefficient	0.35

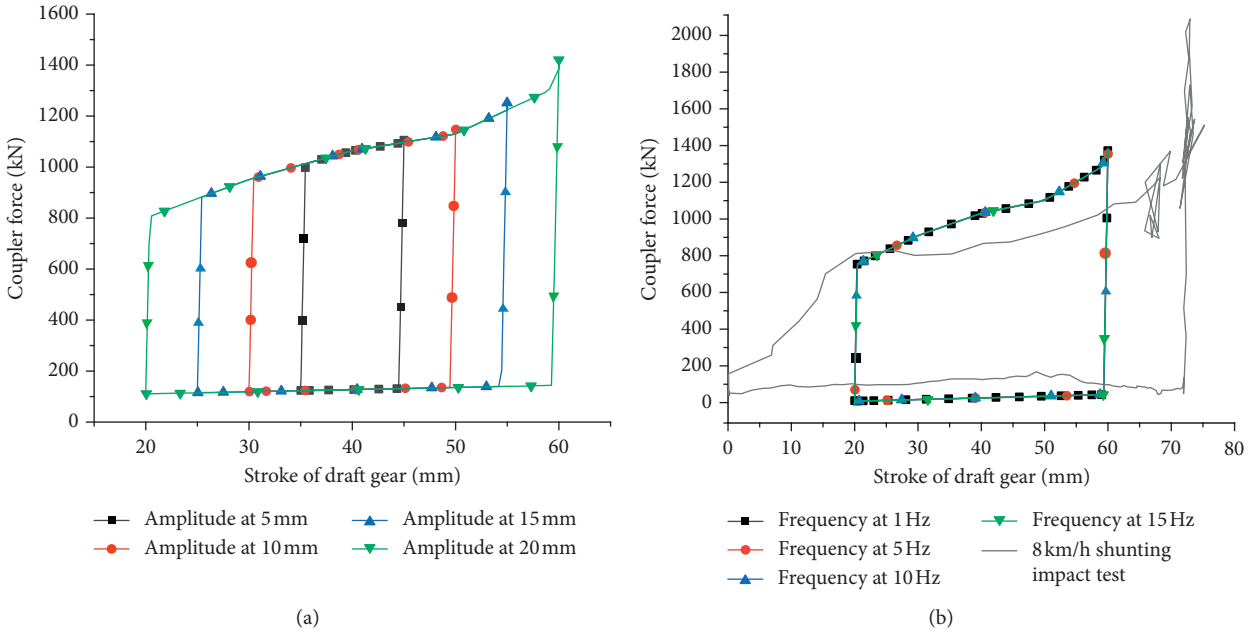

Figure 8: Bench test simulation with the lookup table model. (a) Bench test simulation at different amplitudes. (b) Bench test simulation at different frequencies.

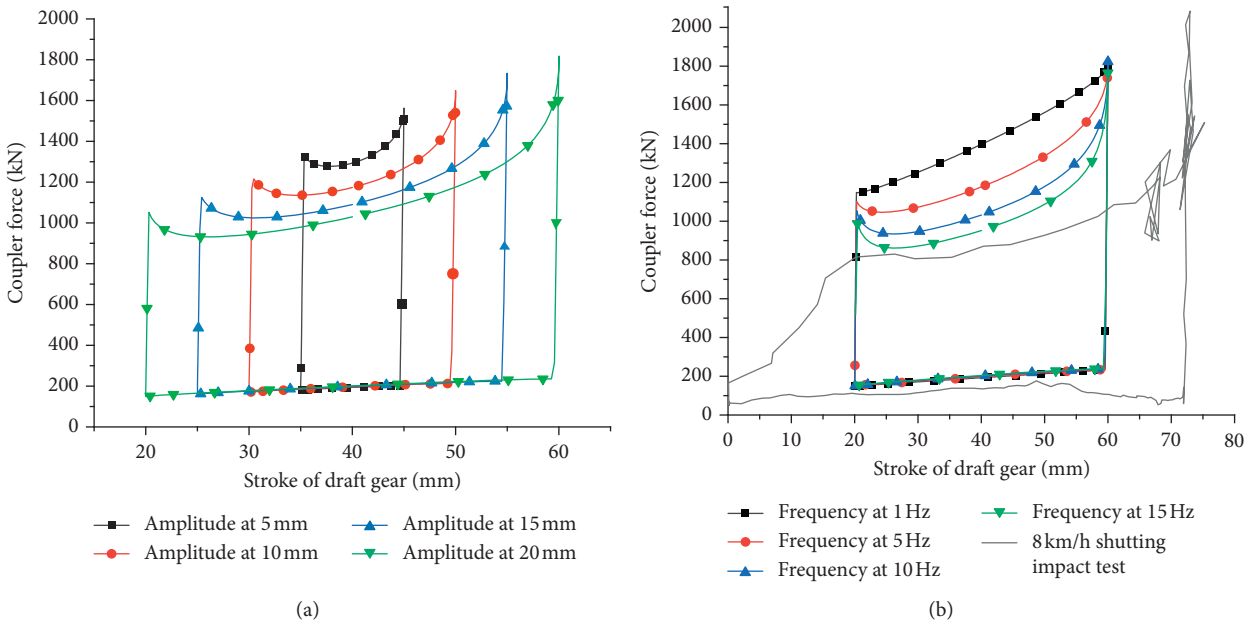

Figure 9: Bench test simulation with the wedge-spring model. (a) Bench test simulation at different amplitudes. (b) Bench test simulation at different frequencies.

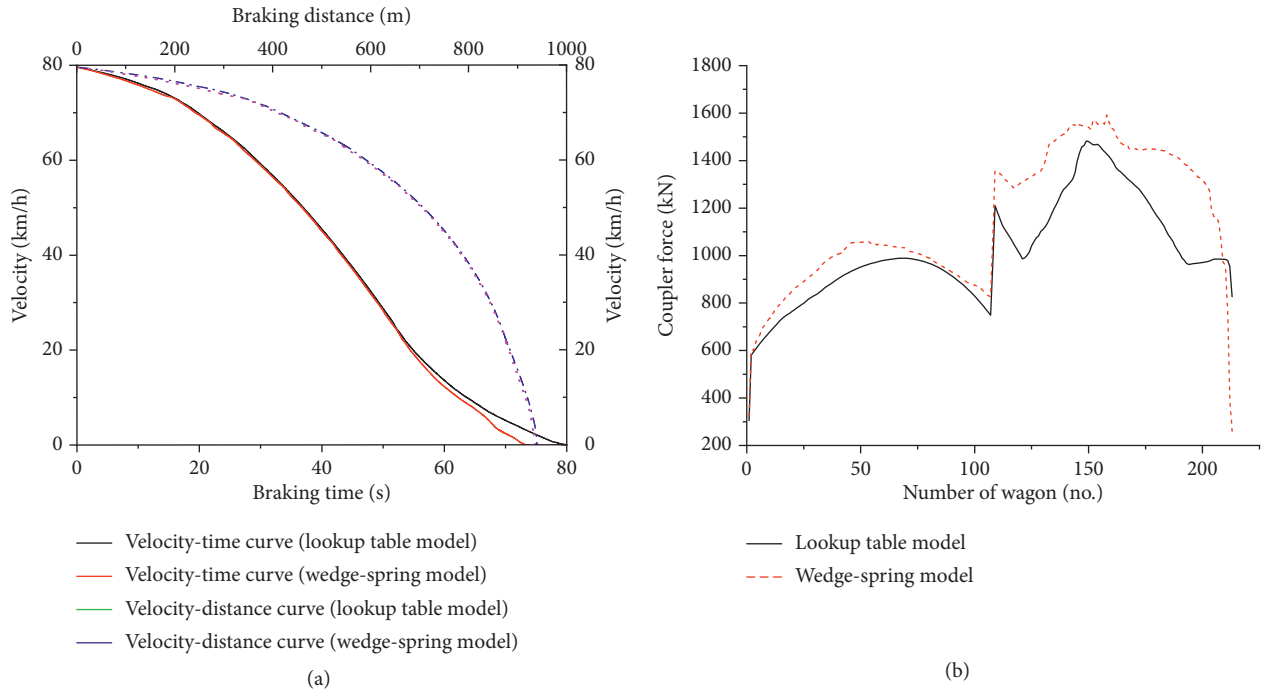

Figure 10: Simulation results of 170 kPa applied full-braking condition. (a) Velocity variation curve. (b) Number of wagon with maximum coupler force.

Table 3: 170 kPa applied full-braking experiment and simulation results.

	Experiment	Lookup table model	Wedge-spring model
Initial braking velocity (km/h)	79.6	79.6	79.6
Braking distance (m)	1083	939	922
Braking time (s)	72.4	79.6	73.1
Maximum coupler force (kN)	1631	1482	1592
Wagon number with maximum coupler force	157	147	156

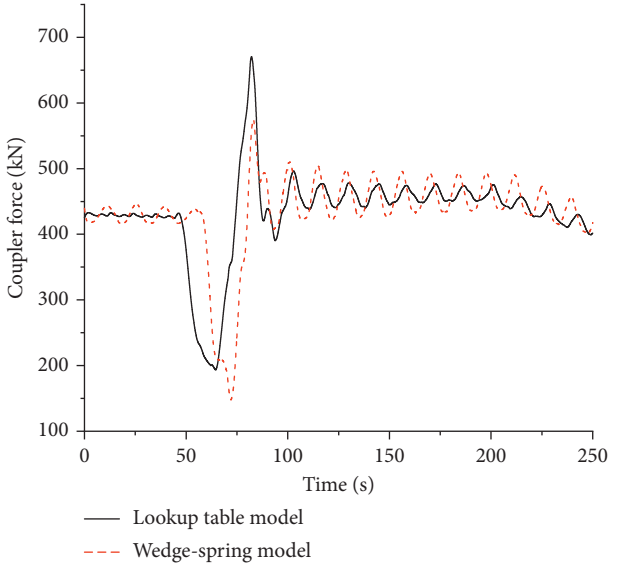

Figure 11: Time course of the coupler force of the 108th wagon.

the longitudinal impulse occurs, the coupler force decreases first and then increases rapidly to the maximum value. The maximum coupler force calculated from the lookup table model is 670.3 kN, while that from the wedge-spring model is smaller, with the maximum value at 580.6 kN. However, the coupler force of the lookup table model decreases rapidly after the maximum value appears, and then the small vibration occurs and gradually converges, whereas after the coupler force of the wedge-spring model reaches the maximum value, the amplitude of the vibration becomes larger and the convergence velocity becomes slower. This feature is mainly caused by the friction characteristics of the draft gear model.

5. Conclusions

(1) The draft gear is divided into four phases during the loading and unloading processes. The quasistatic analysis can be conducted by the force balance condition. The force-displacement curves in the four working phases are linear and continuous, but there

is discontinuity from one working phase to another. In actual shunting or working conditions, the draft gear often has a spike effect at the end of loading and at the beginning of unloading process. The draft gear model can be established by the lookup table method and the simplified wedge-spring method.

(2) For the lookup table model, the simulated draft gear characteristic curve develops along a fixed trajectory under various experimental conditions, regardless of the change rate of the draft gear stroke, while for the wedge-spring model, simulation results depend on the change rate of the draft gear stroke, reflecting the dynamic characteristics of the draft gear and conforming to the law that the friction coefficient is affected by the velocity. Researches show that simulation results of the wedge-spring model in each working condition are more consistent with the experimental results, and thus, this model has better adaptability and wider application.

(3) For the simulation of the full-braking condition on flat straight road, the longitudinal dynamics performance calculated from the wedge-spring model is more accurate. As for the simulation of the longitudinal impulse generated after the air brake of the train, the variation trends of the coupler force curve calculated from different models are basically the same, but the amplitude and frequency of the longitudinal impulse are different.

Data Availability

The data used to support the findings of this study are available from the corresponding author upon request.

Conflicts of Interest

The authors declare that they have no conflicts of interest.

Acknowledgments

The authors thank the National Natural Science Foundation of China (grant no. 51575458) for their aid and support.

References

[1] A. Massa, L. Stronati, A. K. Aboubakr, A. A. Shabana, and N. Bosso, "Numerical study of the noninertial systems: application to train coupler systems," *Nonlinear Dynamics*, vol. 68, no. 1-2, pp. 215–233, 2012.

[2] C. Cole, "Improvements to wagon connection modelling for longitudinal train simulation," in *Proceedings of the Conference on Railway Engineering Proceedings: Engineering Innovation for a Competitive Edge*, pp. 187–194, Central Queensland University, Rockhampton, Australia, September 1998.

[3] F. Cheli and S. Melzi, "Experimental characterization and modelling of a side buffer for freight trains," *Proceedings of the Institution of Mechanical Engineers, Part F: Journal of Rail and Rapid Transit*, vol. 224, no. 6, pp. 535–546, 2010.

[4] T. Geike, "Understanding high coupler forces at metro vehicles," *Vehicle System Dynamics*, vol. 45, no. 4, pp. 389–396, 2007.

[5] Y. Hu, W. Wei, and X. Qi-Wen, "Study of heavy haul freight wagon buffer model based on BP neural network," *Journal of Dalian Jiaotong University*, vol. 33, no. 6, pp. 1–5, 2012, in Chinese.

[6] X. Jin and Y. Luo, "The mathematic description of features of the friction type draft gears," *Rolling Stock*, vol. 49, no. 6, pp. 1–4, 2011, in Chinese.

[7] W.-M. Zhai, "Two simple fast integration methods for large-scale dynamic problems in engineering," *International Journal for Numerical Methods in Engineering*, vol. 39, no. 24, pp. 4199–4214, 1996.

[8] W.-H. Zhang, M. R. Chi, and J. Zeng, "A new simulation method for the train dynamics," in *Proceedings of the 8th International Heave Haul Conference*, pp. 773–778, Rio de Janeiro, Brazil, June 2005.

[9] M. R. Chi, Y.-P. Jiang, W.-H. Zhang, and Y. Wang, "System dynamics of long and heavy haul train," *Journal of Traffic and Transportation Engineering*, vol. 11, no. 3, pp. 34–40, 2011.

[10] S.-L. Sun, L. Fu, Y.-H. Huang et al., "Numerical simulation of railway vehicle impacts," *Journal of Southwest Jiaotong University*, vol. 48, no. 3, pp. 507–512, 2013.

[11] W. Wei and Y. Lin, "Simulation of a freight train brake system with 120 valves," *Proceedings of the Institution of Mechanical Engineers, Part F: Journal of Rail and Rapid Transit*, vol. 223, no. 1, pp. 85–92, 2009.

[12] P. Belforte, F. Cheli, G. Diana, and S. Melzi, "Numerical and experimental approach for the evaluation of severe longitudinal dynamics of heavy freight trains," *Vehicle System Dynamics*, vol. 46, pp. 937–955, 2008.

[13] Q. Wu, M. Spiryagin, and C. Cole, "Advanced dynamic modelling for friction draft gears," *Vehicle System Dynamics*, vol. 53, no. 4, pp. 475–492, 2015.

[14] Q. Wu, S. Luo, T. Qu, and X. Yang, "Comparisons of draft gear damping mechanisms," *Vehicle System Dynamics*, vol. 55, no. 4, pp. 501–516, 2017.

[15] Y. Sun, C. Cole, M. Spiryagin, T. Godber, S. Hames, and M. Rasul, "Longitudinal heavy haul train simulations and energy analysis for typical Australian track routes," *Proceedings of the Institution of Mechanical Engineers, Part F: Journal of Rail and Rapid Transit*, vol. 228, no. 4, pp. 355–366, 2013.

[16] Q. Wu, M. Spiryagin, C. Cole et al., "International benchmarking of longitudinal train dynamics simulators: results," *Vehicle System Dynamics*, vol. 56, no. 3, pp. 343–365, 2018.

[17] Q.-T. Qi, *Analysis and Application of Frictional Draft Gear Dynamic characteristics*, Southwest Jiaotong University, Chengdu, China, 1994.

[18] X. Sun, *Principle and Explanation for Accurate Calculation Program of Train dynamics*, Locomotive and Car Research Institute of Southwest Jiaotong University, Chengdu, China, 1989.